Experimental characterization of a coupled deformation-diffusion theory for elastomeric materials

by

Sterling Watson

Submitted to the Department of Mechanical Engineering
in partial fulfillment of the requirements for the degree of

Bachelor of Science in Mechanical Engineering

at the

MASSACHUSETTS INSTITUTE OF TECHNOLOGY

June 2015

Signature redacted

Author .....
Department of Mechanical Engineering
May 8, 2015

Signature redacted

Certified by .....
Lallit Anand
Warren and Towneley Rohsenow Professor of Mechanical Engineering
Thesis Supervisor

Signature redacted

Accepted by .....
Anette Hosoi
Professor of Mechanical Engineering
Undergraduate Officer

Experimental characterization of a coupled deformation-diffusion theory for elastomeric materials

by

Sterling Watson

Submitted to the Department of Mechanical Engineering
on May 8, 2015, in partial fulfillment of the
requirements for the degree of
Bachelor of Science in Mechanical Engineering

Abstract

Certain cross-liked polymer networks can absorb solvents and swell far beyond their intial volume, a useful property which may be exploited in a variety of applications. In this thesis, polydimethylsiloxane (PDMS) samples were swollen in pentane in order to experimentally characterize the transient and steady-state swelling behavior of this system, and to extract material properties in order to fully characterize a coupled deformation-diffusion theory. Free swelling experiments, transient swelling force measurements, and an analysis of the swollen geometry of a PDMS bilayer strip were performed, and compared to numerical simulations. The experimental results and numerical simulations were shown to be in good agreement.

Thesis Supervisor: Lallit Anand
Title: Warren and Towneley Rohsenow Professor of Mechanical Engineering

Acknowledgments

I would like to acknowledge my advisor, Professor Lallit Anand, for his guidance and advice throughout my undergraduate years, and for the opportunity to work under his supervision on this thesis project. I would also like to thank Claudio Di Leo for the assistance, teaching, and training that he has provided me for this thesis, particularly with the simulations. I am incredibly grateful to both of them for the help, support, and knowledge that they have provided me throughout this endeavor.

Contents

List of Figures

List of Tables

Chapter 1

Introduction

An elastomeric gel is a material composed of a polymer network and solvent. The cross-linked polymer network of a gel can absorb solvents and swell far beyond its initial volume, which is a useful property exploited in a variety of applications, including actuation and sensing in microfluidics, drug delivery and tissue engineering, and channel sealing for oil-fields. The purpose of this thesis was to develop a suite of experiments in order to fully characterize a theory for the coupled deformation-diffusion behavior of swellable gels. For these experiments, polydimethylsiloxane (PDMS) was chosen as the polymer, and pentane was chosen for the solvent.

PDMS is the most widely used silicon-based organic polymer. It was selected for this work because of the ease of manufacturing different cross-linking compositions, simply by combining different ratios of pre-polymer and curing agent. Pentane is one of the least hazardous substances that can induce a large degree of swelling in the PDMS network, and was our solvent of choice for these experiments.

This thesis is organized as follows. In Chapter 2, an overview of the coupled deformation-diffusion theory for swellable elastomers of Chester and Anand is presented. In Chapter 3 we present the experiments performed, their results, and the calibration of the theory based on these experiments. Chapter 4 describes a validation experiment and simulation used to test the theory. And finally, Chapter 5 closes with conclusions and suggestions for future work.

Chapter 2

Summary of the coupled deformation-diffusion theory for swellable elastomers of Chester and Anand

As stated in the introduction, one objective of this work was to develop a suite of experiments in order to fully characterize a theory for the coupled deformation-diffusion behavior of swellable gels. In order to understand the material parameter required, in this section we briefly summarize the continuum theory for elastomeric gels of Chester and Anand, see Chester and Anand (2010, 2011); Chester et al. (2015). The theory relates the following basic fields:

$\mathbf{x} = \boldsymbol{\chi}(\mathbf{X}, t)$,	motion;
$\mathbf{F} = \nabla\boldsymbol{\chi}, \quad J = \det\mathbf{F} > 0$,	deformation gradient;
$\mathbf{F} = \mathbf{F}^e\mathbf{F}^s$,	multiplicative decomposition of $\mathbf{F}$;
$\mathbf{F}^s, \quad J^c = \det\mathbf{F}^s > 0$,	swelling distortion;
$\mathbf{F}^e, \quad J^e = \det\mathbf{F}^e > 0$,	elastic distortion;
$\mathbf{F}^e = \mathbf{R}^e\mathbf{U}^e = \mathbf{V}^e\mathbf{R}^e$,	polar decompositions of $\mathbf{F}^e$;
$\mathbf{C} = \mathbf{F}^\top\mathbf{F}$,	right Cauchy-Green tensor;
$\mathbf{B} = \mathbf{F}\mathbf{F}^\top$,	left Cauchy-Green tensor;
$\bar{\lambda} = \frac{1}{\sqrt{3}}\sqrt{\operatorname{tr}\mathbf{C}}$,	effective stretch;
$\mathbf{T} = \mathbf{T}^\top$,	Cauchy stress;
$\mathbf{T}_{\mathrm{R}} = J\mathbf{T}\mathbf{F}^{-\top}$,	Piola stress;
ψ_{R},	free energy density per unit reference volume;
c_{R},	molar concentration per unit reference volume;
$c = J^{1-}c_{\mathrm{R}}$,	molar concentration per unit deformed volume;
Ω,	volume of a mole of the diffusing species;
μ,	chemical potential;
$\mathbf{j}$,	spatial species flux vector;

2.1 Constitutive equations

1. **Kinematics.** Multiplicative decomposition of the deformation gradient,

$$\mathbf{F} = \mathbf{F}^e\mathbf{F}^s, \tag{2.1.1}$$

with

$$J = \det\mathbf{F} > 0, \quad J^e = \det\mathbf{F}^e > 0, \quad \text{and} \quad J^s = \det\mathbf{F}^s > 0. \tag{2.1.2}$$

The swelling distortion is taken to be spherical

$$\mathbf{F}^s = \lambda^s\mathbf{1}, \tag{2.1.3}$$

with λ^s the swelling stretch. Further, with Ω denoting the volume of a mole of fluid molecules, we assume the swelling stretch to be given by

$$\lambda^s = (1 + \Omega c_{\mathrm{R}})^{1/3}. \tag{2.1.4}$$

2. **Stress.** The Cauchy stress is given by

$$\mathbf{T} = J^{-1}\Big(G_0(\zeta\mathbf{B} - \zeta_0\mathbf{1}) + J^sK(\ln J^e)\mathbf{1}\Big), \tag{2.1.5}$$

where

$$\zeta \stackrel{\text{def}}{=} \left(\frac{\lambda_L}{3\bar{\lambda}}\right)\mathcal{L}^{-1}\left(\frac{\bar{\lambda}}{\lambda_L}\right), \quad \text{and} \quad \zeta_0 \stackrel{\text{def}}{=} \left(\frac{\lambda_L}{3}\right)\mathcal{L}^{-1}\left(\frac{1}{\lambda_L}\right), \tag{2.1.6}$$

and where $\mathcal{L}^{-1}(z)$ is the Langevin inverse function. Here, G_0 is a ground-state shear modulus, K is a bulk modulus, and λ_L is an effective locking stretch. Note that since $\mathcal{L}^{-1}(z) \to \infty$ as $z \to 1$, the stretch-dependent shear modulus $G = G_0\zeta \to \infty$ as $\bar{\lambda} \to \lambda_L$.

3. **Chemical potential.** The chemical potential is given by

$$\mu = \mu^0 + R\vartheta\Big(\ln(1-\phi) + \phi + \chi\phi^2\Big) - \Omega K(\log J^e) + \frac{1}{2}\Omega K(\log J^e)^2, \tag{2.1.7}$$

where ϕ is the polymer volume fraction defined as

$$\phi \stackrel{\text{def}}{=} \frac{1}{1 + \Omega c_{\mathrm{R}}} = (\lambda^s)^{-3} = (J^s)^{-1}. \tag{2.1.8}$$

4. **Species flux. Mobility.** The spatial species flux is prescribed a constitutive equation of the form

$$\mathbf{j} = -m\,\mathrm{grad}\,\mu, \tag{2.1.9}$$

where the mobility m is given by

$$m = \frac{D_0 c}{R\vartheta}, \tag{2.1.10}$$

with D_0 the self diffusivity of the fluid in the polymer.

2.2 Governing partial differential equations

The governing partial differential equations, when expressed in the deformed body, consist of

1. The local force balance for the Cauchy stress,

$$\mathrm{div}\mathbf{T} + \mathbf{b} = \mathbf{0}, \tag{2.2.1}$$

where $\mathbf{b}$ is a non-inertial body force, and $\mathbf{T}$ is given by (2.1.5).

2. The local balance for the fluid concentration,

$$\dot{c}_{\mathrm{R}} = -J\,\mathrm{div}\mathbf{j}, \tag{2.2.2}$$

where the flux $\mathbf{j}$ is given by (2.1.9), and the chemical potential is given by (2.1.7).

The theory summarized in Sections 2.1 and 2.2 requires six material parameters as listed in Table 2.1.

G_0	Elastic Properties
λ_L	
K	
Ω	Fluid Properties
D_0	
χ	Network & Fluid Properties

Table 2.1: Material properties for the fully-coupled deformation-diffusion theory for swellable elastomers.

Next we describe the experiments performed to determine the material parameters listed in Table 2.1 for the theory summarized in this section.

Chapter 3

Experimental calibration of the theory

In this work we have chosen to calibrate the theory to one specific elastomer/solvent system. As the elastomer we have chosen polydimethylsiloxane (PDMS), and as the solvent we have chosen pentane. PDMS was chosen since it is simple to manufacture and since its mechanical properties can be modified by varying the preparation procedure used. PDMS is manufactured by mixing a prepolymer with a curing agent at a particular mass ratio. In this work we will consider the mass ratios

$$10{:}1, \quad 15{:}1, \quad \text{and} \quad 20{:}1,$$

which, as shown in the following sections, lead to significantly different mechanical properties. Pentane was chosen as a solvent since it readily diffuses into PDMS and causes a large degree of swelling. The volume of a mole of fluid molecules Ω, and the self diffusivity of the fluid D_0 are material properties of the fluid only. From Hu et al. (2011), for pentane we have that

$$\begin{aligned} \Omega &= 1.15 \cdot 10^{-4}\,\mathrm{m}^3/\mathrm{mol} \\ D_0 &= 5.45 \cdot 10^{-9}\,\mathrm{m}^2/\mathrm{sec} \end{aligned} \tag{3.0.1}$$

In order to characterize all other material properties in the theory, we use data from three experiments:

1. Mechanical tension tests on the dry PDMS samples;
2. Mass measurements of freely-swollen samples;
3. Constrained swelling experiments.

The mechanical tension tests were performed by Huang and Anand (2005, 2015), and we use their data here. We note that the procedure for preparing PDMS samples summarized below is *identical* to that used by Huang and Anand.

3.1 Preparation of PDMS for swelling experiments

An aluminum mold, shown in Figure 3-1, was used to make cylindrical PDMS samples of height 0.5 inches and diameter 0.5 inches. Cylindrical samples composed of different mass

ratios of prepolymer and curing agent were prepared using the following procedure:

1. Prepare mold by affixing squares of aluminum sheet to the back using electrical tape, to create removable backing for demolding PDMS samples.
2. Combine prepolymer and curing agent, and mix in Thinky mixer using a 1 minute, 2000 rpm degas mixing procedure.
3. Pour samples into mold, and degas for 45 minutes, until samples are free of bubbles.
4. Place mold into the oven, and cure at 100°C for 7 days.

An initial problem with the sample preparation procedure was leaking of the PDMS through the mold during the degassing and curing procedures, which caused samples to be shorter than the desired 0.5 inch height, with a concave upper surface. This problem was resolved by spacing out the samples in the mold such that the aluminum squares could be taped securely, without overlap. The mold was also slightly overfilled so that the samples would have a flat upper surface when cured.

The seven day curing time was selected to match the experimental procedures of Huang and Anand (2015). As noted by Huang and Anand, the mechanical properties of PDMS continue to vary with increasing curing time. As such, a consistent experimental procedure is important is crucial in the preparation of PDMS samples.

3.2 Mechanical tension tests of Huang and Anand

Huang and Anand (2015) performed mechanical tension tests on tensile specimens based on a 1/3 scale of the tension specimen geometry specified by ASTM-D412, cf. Figure 3-2(a). A typical tension specimen is shown in Fig. 3-2(b). Tension experiments were conducted on a Zwick/Roell testing machine at a crosshead speed of 50 mm/min. Stretch in the gauge sections of the specimens was measured using digital image correlation (DIC) by tracking two black dots on the gauge section. The readings were converted to engineering stress versus stretch curves using the dimensions of each specimen in the gauge section, and assuming that the PDMS is incompressible. The experimental data (symbols) is shown in Figure 3-3 for 10:1, 15:1, and 20:1 compositions.

Considering a simple extension deformation

$$\lambda_1 = \lambda, \quad \lambda_2 = \lambda_3 = \lambda^{-1/2}, \quad \bar{\lambda} = \frac{1}{\sqrt{3}}\sqrt{\lambda^2 + 2\lambda^{-1}},$$

the engineering stress $S = (\mathbf{T}_{\mathrm{R}})_{11}$, may be written as a function of the stretch λ through (cf. Huang and Anand, 2005)

$$S = G(\lambda - \lambda^{-2}), \tag{3.2.1}$$

where the stretch-dependent shear modulus G is given by

$$G = G_0 \left(\frac{\lambda_L}{3\bar{\lambda}}\right) \mathcal{L}^{-1}\left(\frac{\bar{\lambda}}{\lambda_L}\right). \tag{3.2.2}$$

Using (3.2.1) and (3.2.2), the experimental results (symbols) shown in Figure 3-3 were fit using a least squares solver in Matlab to obtain G_0 and λ_L for the various compositions. The results are shown in Table 3.1.

Composition	G_0	λ_L
10:1	0.6347 MPa	1.2055
15:1	0.6272 MPa	1.3009
20:1	0.4913 MPa	1.4148

Table 3.1: Ground state shear modulus G_0 and locking stretch λ_L values for 10:1, 15:1, and 20:1 PDMS compositions.

3.3 Mass measurements of freely-swollen samples.

In these experiments, PDMS samples of varying composition were allowed to swell freely in pentane, after which their mass was measured. The detailed procedure is summarized in what follows: First, the dry mass of each sample was recorded using a Denver Instruments SI-114 analytical balance, and then the samples were placed in a sealed container with pentane (note that PDMS does not float in pentane) for 24 hours. The mass of the swollen samples was then recorded. Care was taken to measure the mass of the swollen samples immediately after removal from the pentane in order to minimize losses due to evaporation. The dry and fully-swollen mass measurements are listed in Table 3.2.

composition	dry mass m_i	fully-swollen mass m_f
10:1	1.4851	2.49
	1.6437	2.75
	1.6553	2.76
15:1	1.2319	2.57
	1.629	3.34
20:1	1.379	3.64
	1.5006	3.99
	1.6126	4.26

Table 3.2: Mass measurements for 10:1, 15:1, and 20:1 PDMS samples, before and after free swelling in pentane for 24 hours.

Using the dry mass m_i and the fully-swollen mass m_f, along with the mass densities of

PDMS ρ_{PDMS} and pentane ρ_{pen}, we may calculate the dry volume of PDMS as

$$V_{0,\text{PDMS}} = \frac{m_i}{\rho_{\text{PDMS}}} \tag{3.3.1}$$

and the volume of pentane in the fully-swollen sample as

$$V_{\text{pen}} = \frac{m_f - m_i}{\rho_{\text{pen}}}. \tag{3.3.2}$$

Assuming **incompressibility** of the PDMS, we have that the swollen volume of PDMS V_{PDMS} is equal to its dry volume, that is $V_{\text{PDMS}} = V_{0,\text{PDMS}}$. With such an assumption we may write the experimentally measured volume ratio as

$$J = \frac{V}{V_0} = \frac{V_{0,\text{PDMS}} + V_{\text{pen}}}{V_{0,\text{PDMS}}} \tag{3.3.3}$$

Further, since we are assuming incompressibility of the PDMS, all volume deformation is due to swelling and, recalling (2.1.8), we may write

$$J = \lambda^3 = (\lambda^s)^3 = J^s = \phi^{-1} \tag{3.3.4}$$

Averaging the dry mass m_i, and fully-swollen mass m_f experimental measurements shown in Table 3.2, and using

$$\begin{aligned} \rho_{\text{PDMS}} &= 970\,\text{kg/m}^3, \quad \text{from Mark (1998), and} \\ \rho_{\text{pen}} &= 626\,\text{kg/m}^3, \quad \text{from Sigma-Aldrich (2015).} \end{aligned} \tag{3.3.5}$$

we may compute the experimentally measured steady-state volume ratio J_{ss}, steady-state polymer volume fraction ϕ_{ss}, and steady-state stretch λ_{ss} using (3.3.1) through (3.3.4). These results are shown in Table 3.3.

composition	J_{ss}	ϕ_{ss}	λ_{ss}
10:1	2.0418	0.4898	1.2686
15:1	2.6553	0.3766	1.3847
20:1	3.5517	0.2816	1.5257

Table 3.3: Experimentally-measured values of steady-state volume ratio J_{ss}, steady-state polymer volume fraction ϕ_{ss}, and steady-state stretch λ_{ss} for 10:1, 15:1, and 20:1 PDMS compositions.

Remark. In isotropic free-swelling, at steady-state, $\lambda_1 = \lambda_2 = \lambda_3 = \lambda_{\text{ss}}$, and $\bar{\lambda}_{\text{ss}} = \lambda_{\text{ss}}$. Using this we may compare the effective locking stretch measured from the mechanical tests and listed in Table 3.1, with the effective steady-state stretch $\bar{\lambda}_{\text{ss}}$ measured from the free swelling experiments as shown below

composition	λ_L	$\bar{\lambda}_{\text{ss}}$
10:1	1.2055	1.2686
15:1	1.3009	1.3847
20:1	1.4148	1.5257

For all compositions we have the discrepancy that $\bar{\lambda}_{\text{ss}} > \lambda_L$. This situation is in some sense "unphysical", since for the material model chosen here, the material is not allowed to deform to effective stretches above the locking stretch. We believe this discrepancy might arise from one (or both) of two following reasons:

- First, it is possible that the introduction of pentane into the PDMS polymer **increases the locking length** by interacting with the polymer chains.

- It is possible that the PDMS polymer is not incompressible when swollen.

In order to use the free-swelling experiments developed here to characterize the interaction parameter χ appearing in the chemical potential (2.1.7), we will assume that locking length λ_L is increasing when the PDMS is being swollen with pentane. The specific values used are listed in what follows. □

Following Chester and Anand (2010), we now apply the model, under incompressible conditions, to the modeling isotropic equilibrium free swelling. Under such conditions, the deformation gradient $\mathbf{F}$ has the simple form

$$\mathbf{F} = \lambda \mathbf{1} = \phi^{-1/3}\mathbf{1}. \tag{3.3.6}$$

For an incompressible material, the Cauchy stress (2.1.5) is given by

$$\mathbf{T} = J^{-}1\Big(G_0\zeta\mathbf{B} - P\mathbf{1}\Big), \tag{3.3.7}$$

where P is a pressure which must be determined from boundary conditions. Using (3.3.6) and the fact that we are considering stress-free swelling in (3.3.7) yields

$$G_0\zeta\phi^{-2/3} - P = 0, \quad \longrightarrow \quad P = G_0\zeta\phi^{-2/3}. \tag{3.3.8}$$

The chemical potential for an incompressible material may be written as

$$\mu = \mu^0 + R\vartheta\Big(\ln(1-\phi) + \phi + \chi\phi^2\Big) - \Omega G_0\phi + \Omega P\phi, \tag{3.3.9}$$

which using (3.3.8) yields

$$\mu = \mu^0 + R\vartheta\Big(\ln(1-\phi) + \phi + \chi\phi^2\Big) + \Omega G_0(\zeta\phi^{1/3} - \phi). \tag{3.3.10}$$

Finally, swelling-equilibrium is reached when the chemical potential throughout the gel

reaches the chemical potential μ^0 which yields that (3.3.10) may be written as

$$R\vartheta\Big(\ln(1-\phi_{ss})+\phi_{ss}+\chi\phi_{ss}^2\Big)+\Omega G_0(\zeta\phi_{ss}^{1/3}-\phi_{ss})=0, \tag{3.3.11}$$

with

$$\zeta=\left(\frac{\lambda_L}{3\bar{\lambda}_{ss}}\right)\mathcal{L}^{-1}\left(\frac{\bar{\lambda}_{ss}}{\lambda_L}\right).$$

For a given steady-state polymer volume fraction ϕ_{ss}, and with the elastic properties G_0 and λ_L determined, we may solve (3.3.11) for the interaction parameter χ.

As mentioned in the remark following Table 3.3, in order to fit for the parameter χ using (3.3.11), we will assume that the locking length λ_L has increased from the value measured during the mechanical tests. Specifically, we will use a locking length 15% larger than the steady state effective stretch measured through the mass swelling experiments, that is

$$\lambda_L=1.15\cdot\bar{\lambda}_{ss},$$

with the values for $\bar{\lambda}_{ss}$ given in Table 3.3. The χ values determined using (3.3.11) are shown in Table 3.4 along with the parameters G_0, λ_L, and ϕ_{ss} used for fitting. Note that the value for Ω is a known property of the fluid and given in (3.0.1).

composition	parameters used for fitting	resulting χ value
10:1	$G_0=0.6347\,\text{MPa}$ $\lambda_L=1.15\cdot\bar{\lambda}_{ss}=1.4589$	0.5220
15:1	$G_0=0.6272\,\text{MPa}$ $\lambda_L=1.15\cdot\bar{\lambda}_{ss}=1.5924$	0.2921
20:1	$G_0=0.4913\,\text{MPa}$ $\lambda_L=1.15\cdot\bar{\lambda}_{ss}=1.7546$	0.1126

Table 3.4: Interaction parameter χ determined using steady-state polymer volume fraction ϕ_{ss}, and elastic properties G_0 and λ_L.

3.4 Swelling against a flexure

To measure the transient swelling of PDMS in pentane, a cylindrical PDMS samples was allowed to swell against a flexure of spring constant 0.25 N/mm, and the displacement of the structure was recorded over time using a time-lapse camera and digital image correlation. Figure 3-4 shows the experimental setup. Porous metal platens were placed above and below the sample to allow for bubbles to escape and to prevent suction. A lid was used to minimize the evaporation of the pentane during the experiment. An image of the experiment was recorded every 15 seconds for the first ten minutes, and then every minute for 16 additional hours. An image from the experiment, and a schematic of the experimental setup are shown

in Figures 3-5 and 3-6.

This experiment was performed on 10:1, 15:1 and 20:1 composition PDMS samples. Digital image correlation was used to track the vertical displacement of four different points on the flexure. The displacement data was converted into a force versus time plot, and is compared for the three different compositions in Figure 3-8.

In the 20:1 flexure swelling experiment, the PDMS sample did not reach steady state within the 16 hour period used for our analysis. However, when the sample was given enough time to reach steady state, it bottomed out the spring in the flexure setup. The 10:1 and 15:1 samples did reach steady state within the 16 hour period, and did not bottom out the spring because of their smaller steady-state volume.

3.4.1 Finite-element simulations of swelling against a flexure

A finite-element implementation of the deformation-diffusion theory summarized in Section 2, was used to model the transient swelling of PDMS against a flexure. For conciseness, the entire set of material parameters used in the simulation, for each composition of PDMS, is listed in Table 3.5. In all simulations, in order to simulate an almost incompressible material, we take the bulk modulus to be $K = 100 \cdot G_0$.

composition	G_0	λ_L	χ		
10:1	0.6374 MPa	1.4589	0.5220	with	$\Omega = 1.15 \cdot 10^{-4}\,\mathrm{m}^3/\mathrm{mol}$
15:1	0.6272 MPa	1.5924	0.2921		$D_0 = 5.45 \cdot 10^{-9}\,\mathrm{m}^2/\mathrm{sec}$
20:1	0.4913 MPa	1.7546	0.1126		

Table 3.5: Material properties used in the finite-element simulations for various PDMS compositions.

For computational efficiency, we model the problem as axisymmetric as shown in Fig. 3-9. With respect to this figure:

- The axisymmetric cross section of the cylindrical sample sits between two analytical rigid surfaces. The bottom analytical surface is fixed in place, while the top analytical surface is fixed to a single linear-elastic element.
- Frictionless contact conditions are applied between the PDMS sample and the rigid surfaces.
- The experimental flexure is modeled through a single linear-elastic element whose elastic stiffness is set in order to model the flexure stiffness of $k = 0.25\,\mathrm{N/mm}$.
- In order to model the chemical boundary condition of the PDMS exposed to the liquid pentane, we apply a chemical boundary condition to all exterior faces of the simulation domain. The chemical potential on these surfaces is ramped from an initial value μ_i to the chemical potential of the fluid μ^0 in 1000 seconds and is then held constant at μ^0 for 16 hours.

Fig. 3-10 shows contours of polymer volume fraction ϕ for the simulation of 20:1 PDMS at $t \in [0, 0.5, 1, 15]$ hours. Finally, the experimental and simulated force versus time curves are shown in Fig. 3-11, where the simulated data has been shifted in time by 1000 seconds to account for the finite rate at which the chemical potential is applied in the simulation. The simulated results are in reasonably good agreement with the experimental measurements. There are some discrepancies in the steady-state force measurements, especially for the 15:1 and 20:1 compositions. This could potentially be attributed to the uncertainty in the fitting of the locking stretch λ_L.

In order to better compare whether the simulation is capturing the transient swelling behavior, in Fig. 3-12 we shift the simulated force versus time data such that the steady-state force measurements match. It is clear that there is some discrepancy between the simulated results and the experiments in capturing the transient swelling response. Further, this discrepancy seems to be bigger for the PDMS samples with lower pre-polymer to curing-agent ratio. This might potentially indicate that the mobility function (2.1.10) is a function of deformation.

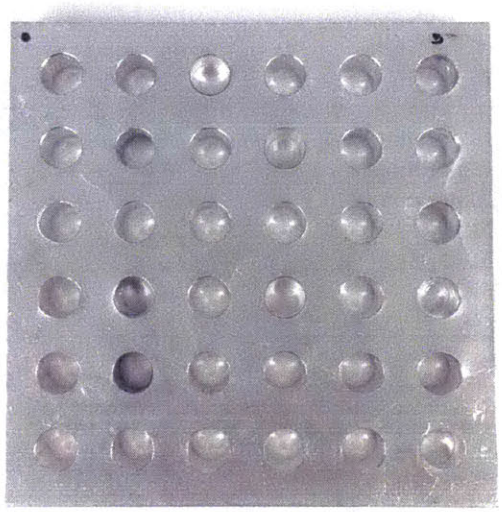

Figure 3-1: Aluminum mold used for creating cylindrical PDMS samples of 0.5 inch height and diameter.

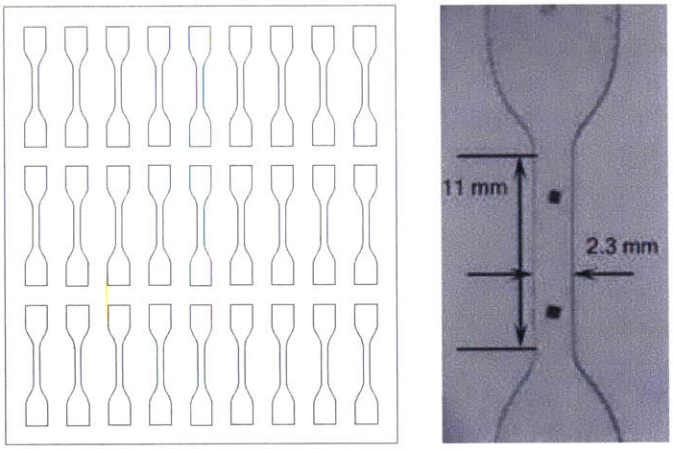

(a) (b)

Figure 3-2: Tension specimen geometry.

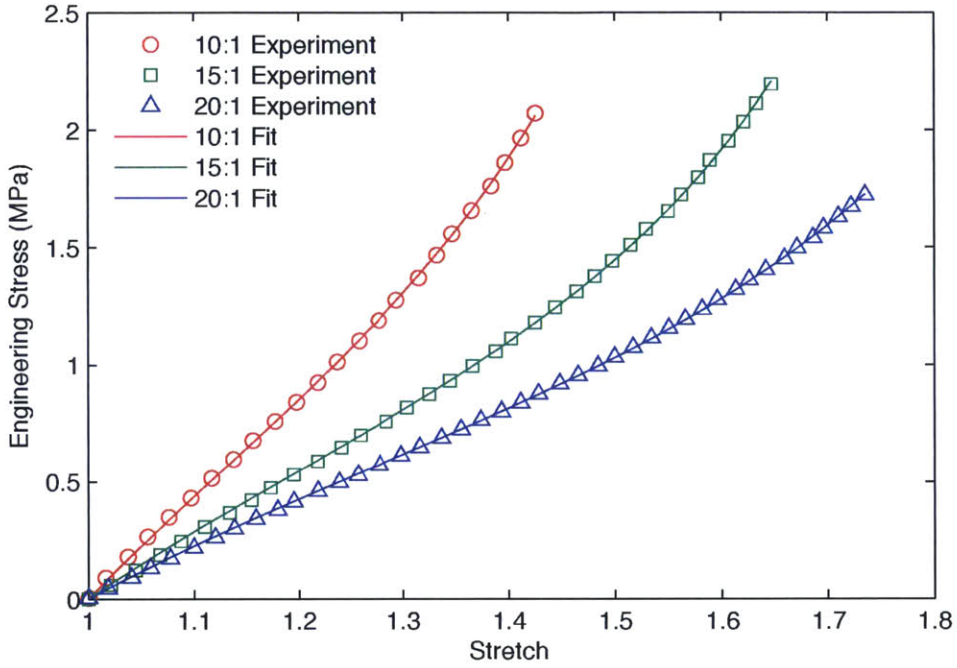

Figure 3-3: Experimental data from tension tests for 10:1, 15:1, and 20:1 composition PDMS samples, and fitted stress-stretch curves.

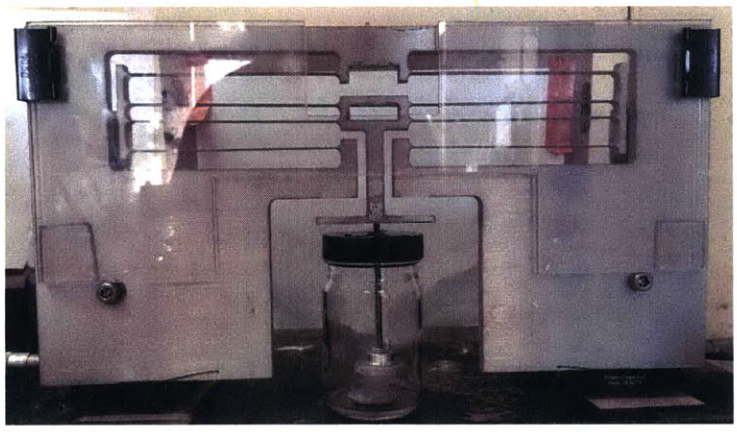

Figure 3-4: Setup for flexure swelling experiments. PDMS samples of 10:1, 15:1, and 20:1 compositions were allowed to swell against an aluminum flexure with spring constant 0.25 N/mm over a period of 16 hours.

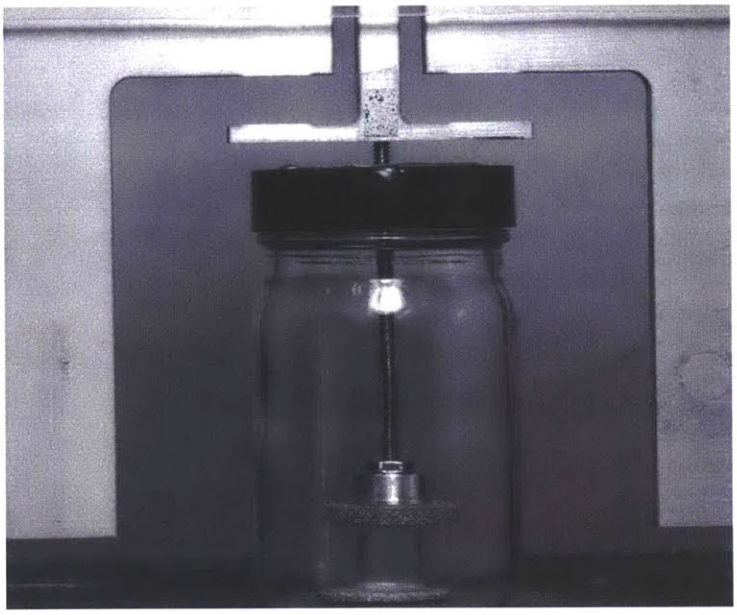

Figure 3-5: Image used in flexure swelling experiment for tracking spring displacement over time. This image was taken prior to adding pentane to the container.

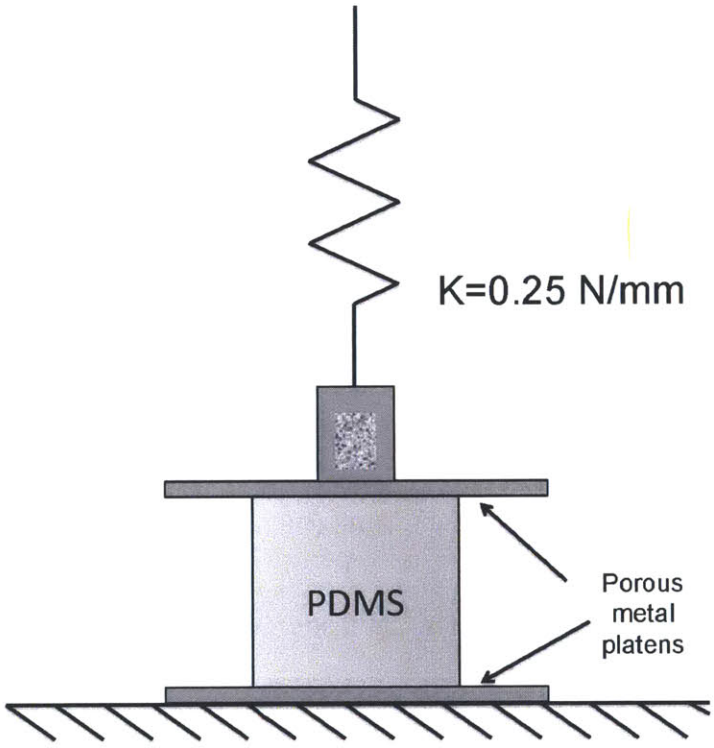

Figure 3-6: Schematic of the flexure swelling experiment setup. The cylindrical PDMS sample was allowed to swell in pentane against a flexure of spring constant 0.25 N/mm.

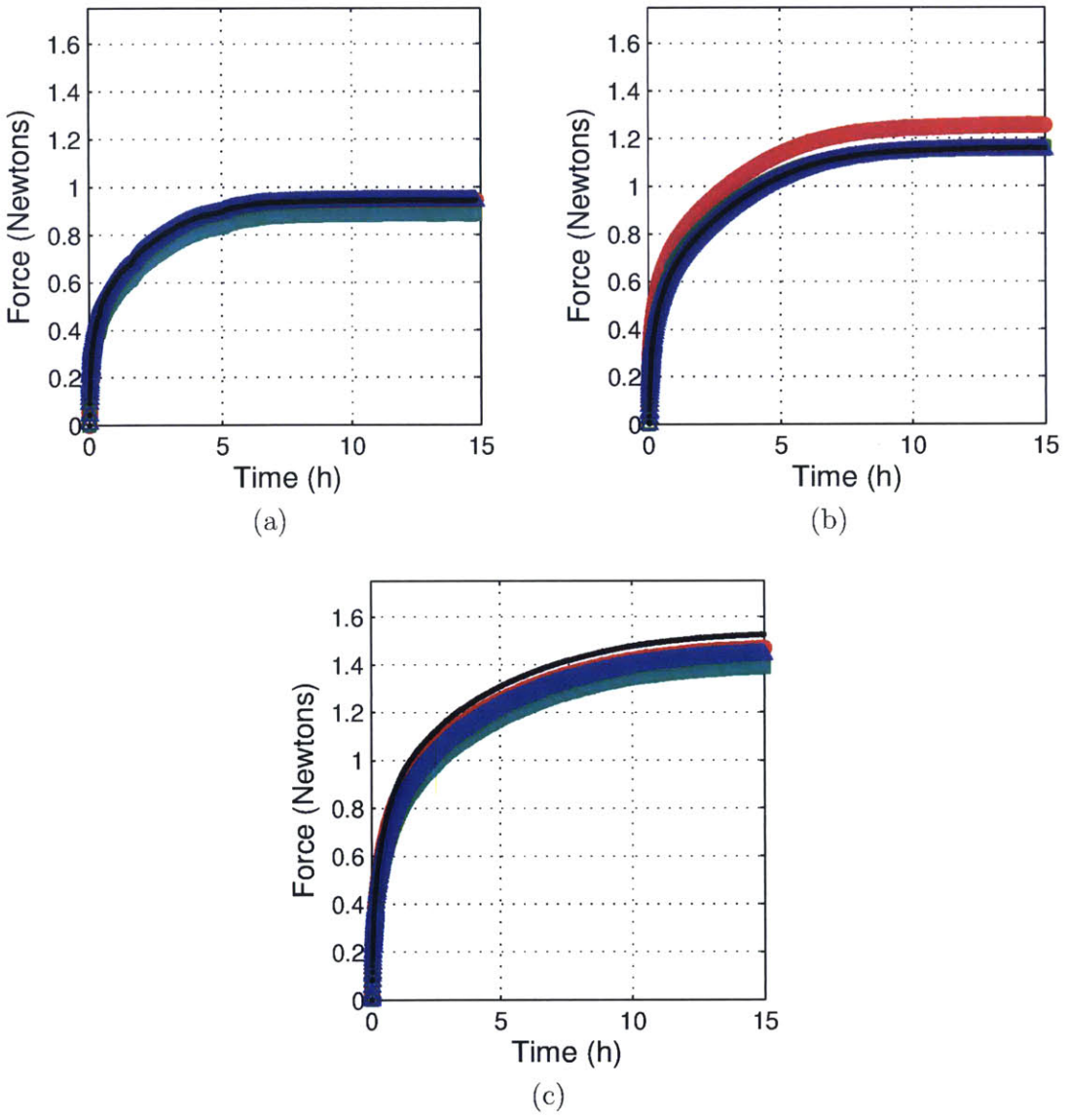

(a) (b)

(c)

Figure 3-7: Force versus time curves for the flexure swelling experiment, for (a) 10:1, (b) 15:1, and (c) 20:1 PDMS compositions.

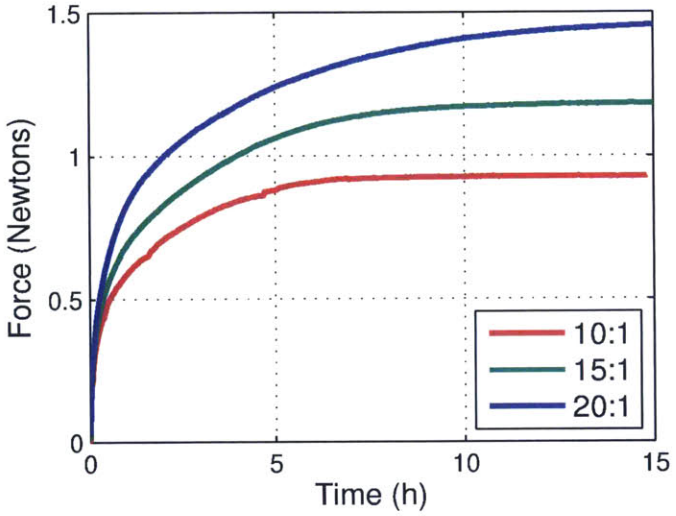

Figure 3-8: A comparison of the force applied to the flexure over time for the three PDMS samples. Applied force and time to reach steady state both increase as the amount of cross-linking decreases.

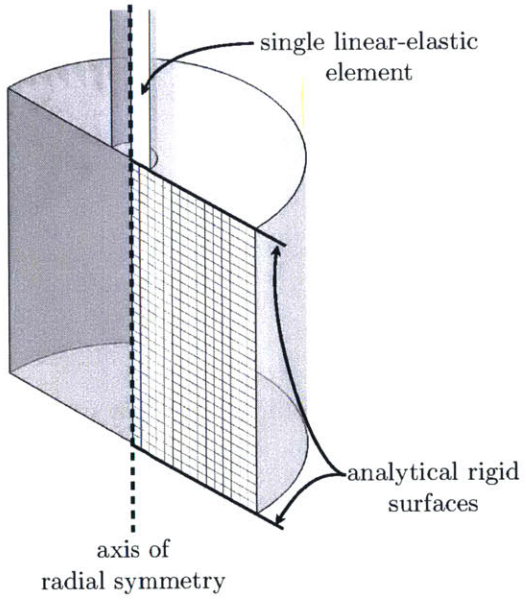

Figure 3-9: Simulation geometry of a PDMS sample.

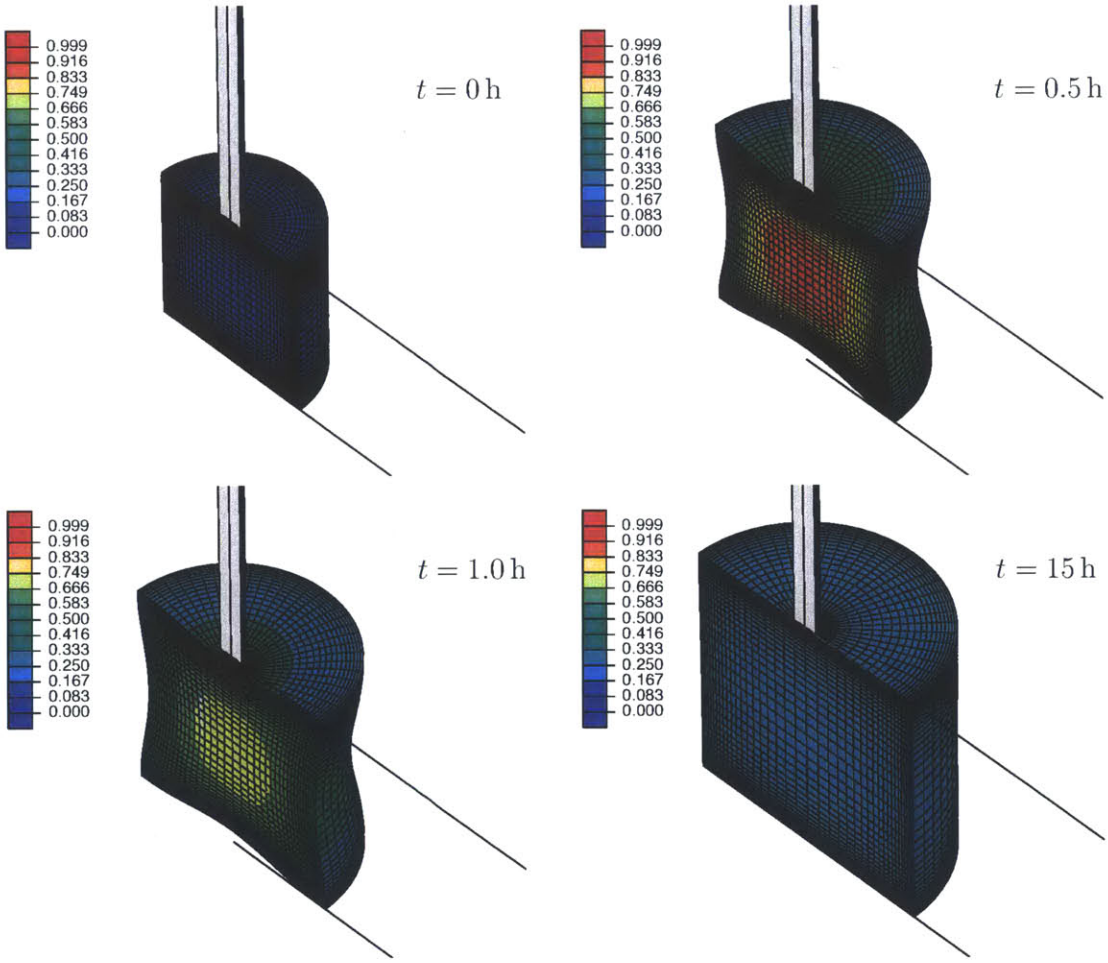

Figure 3-10: Simulation of PDMS swelling against a single linear-elastic element.

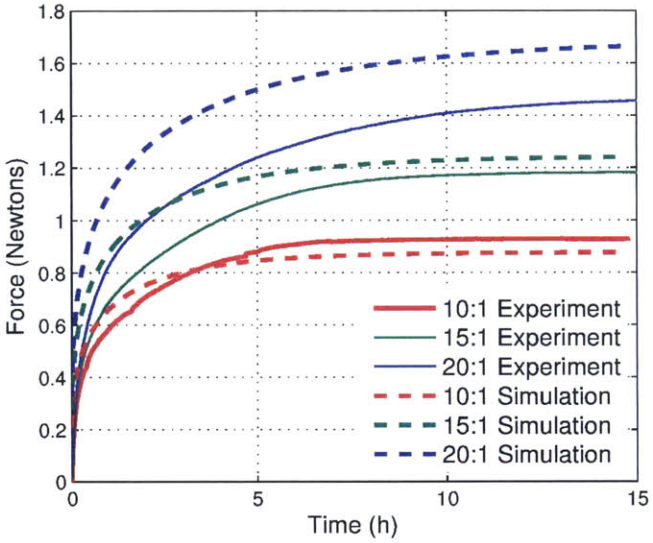

Figure 3-11: Experimental force versus time curves and simulation curves for 10:1, 15:1, and 20:1 PDMS samples.

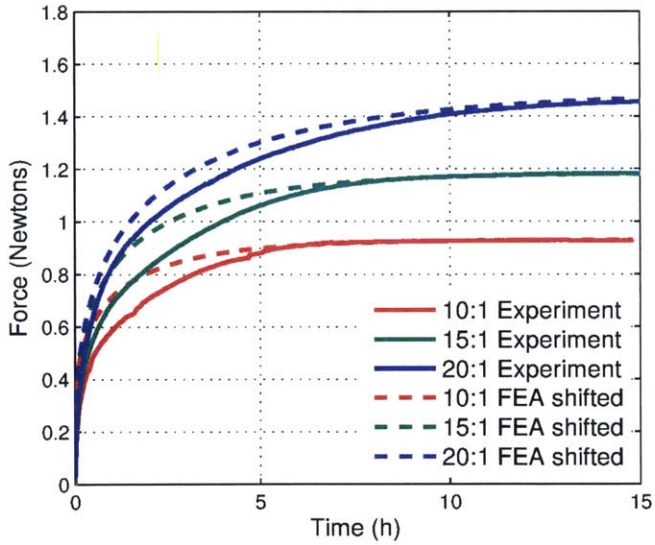

Figure 3-12: FEA curves shifted to match endpoints of experimental data.

Chapter 4

Bilayer swelling validation experiment and simulation

As a potential validation experiment, we consider the swelling of bilayers where each of the two layers is made from PDMS of different compositions. The preparation, testing, and simulation of such bilayers is discussed next.

4.1 Bilayer strip sample preparation

The samples were prepared using the following procedure:

1. Combine and mix 20:1 and 10:1 ratio PDMS in the Thinky mixer, mixing in separate color silicone dyes for identification.
2. Pour the 20:1 dyed PDMS into a disposable plastic petri dish, degas, and cure for 15 minutes at 100°C.
3. Pour the 10:1 dyed PDMS onto the cured 20:1 layer, degas, and let cure for an additional 30 minutes at 100°C.
4. Break plastic petri dish to remove PDMS bilayer disk, and cut PDMS into strips. PDMS bilayer strips are shown in Figure 4-1.

4.2 Bilayer strip curvature

Prior to swelling, the strips' length, width, and layer thicknesses were measured. The strips were allowed to swell fully, and were photographed in their swollen state, as shown in Figure 4-2. To measure the experimental radius of curvature ρ_{exp}, a circle was fitted to the image of the swollen bilayer strip using ImageJ analysis software. The measured radii of curvature are shown in Table 4.1.

The bilayer swelling experiments were simulated using the finite-element implementation of the deformation-diffusion theory summarized in Sect. 2. The material parameters are listed in Tab. 3.5. The steady-state contours of polymer volume fraction for the three bilayer

strips simulated are shown on the right column in Fig. 4-2. The simulated radii of curvature ρ_{fea} were measured in the same fashion as the experimental ones, by fitting a circle to the image of the simulated swollen bilayer strips using ImageJ analysis software. The results are reported in Table 4.1.

The finite-element simulated radii of curvature are in reasonably good agreement with the experimental measurements, but there are some discrepancies. Some potential reasons for the discrepancies are discussed next.

- The simulation was done assuming plane strain, which was not entirely accurate since the strips had finite width and swelled such that they had a finite radius of curvature along their width as well as length.
- The layer uniformity within each strip was also not perfectly consistent throughout the length and width of each strip, which could also contribute to this discrepancy.
- Small errors in the experimental measurements of the thicknesses of each layer would lead to large errors in the radius of curvature.

Strip	10:1 Thickness	20:1 Thickness	Strip Length	ρ_{exp}	ρ_{fea}
1	2.13	2.51	31.02	25.84	23.33
2	2.43	2.11	28.78	25.84	21.77
3	1.78	2.86	38.16	25.05	24.09

Table 4.1: Resulting curvature for swollen bilayers, experimental and simulated.

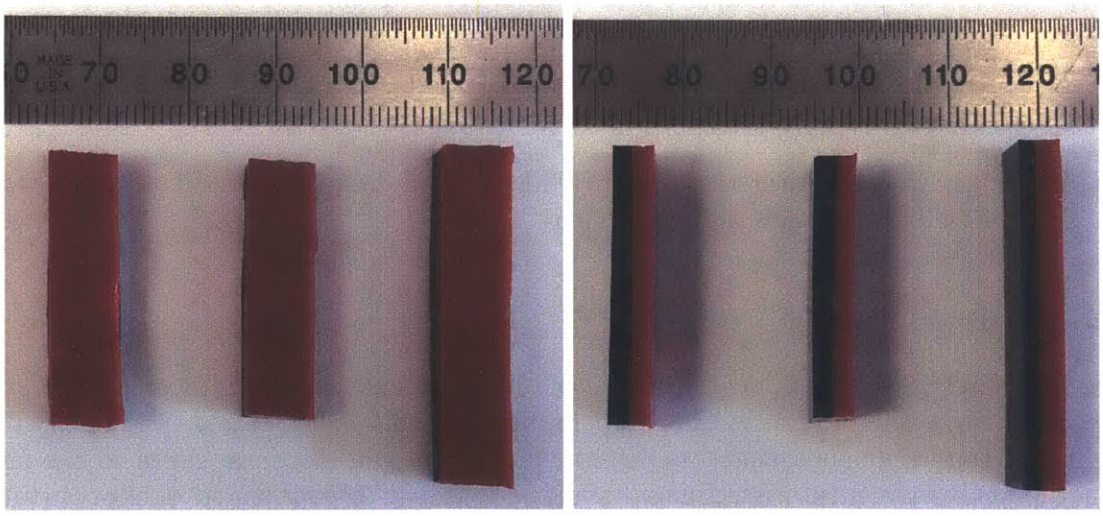

Figure 4-1: Dry PDMS bilayer strips.

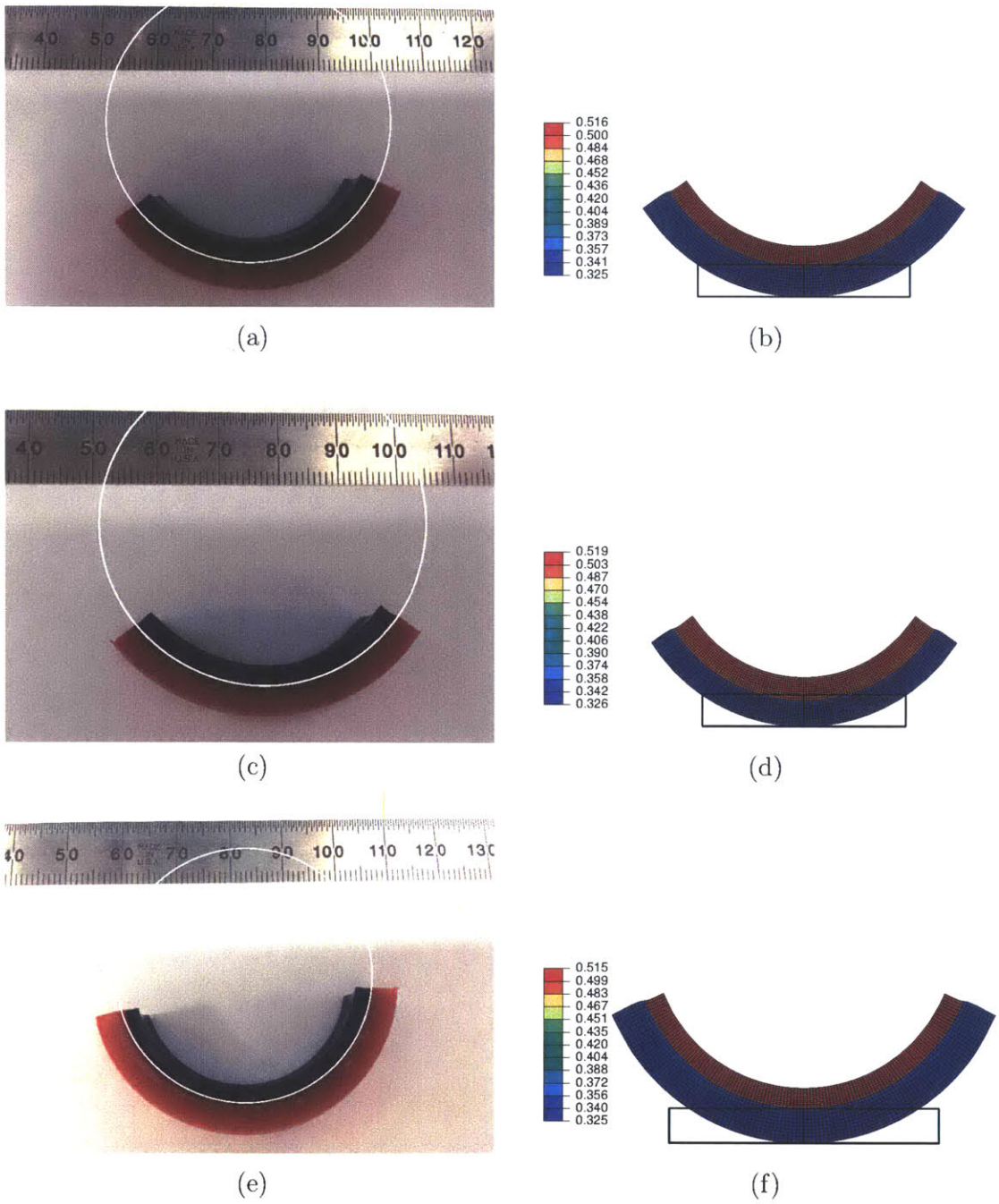

Figure 4-2: On the left, the swollen PDMS bilayer strips, with circles fitted for curvature measurement. The red side is the 20:1 PDMS, and the blue side is the 10:1 PDMS. On the right, FEA simulations of swollen bilayer strips, with the rectangular box indicating initial size and shape.

Chapter 5

Conclusions and future work

For this research, cylindrical PDMS samples were manufactured using prepolymer-to-curing agent ratios of 10:1, 15:1, and 20:1, and were placed in pentane for a series of experiments examining the transient and steady-state swelling behavior. The material parameters obtained by dry polymer tension tests and free swelling volume uptake were used to calibrate the coupled deformation-diffusion theory for swellable elastomers of Chester and Anand. A finite element implementation of the theory was used to simulate experimental measurements of transient swelling of PDMS against a flexure.

A conflict in the model arose when comparing the measured effective locking stretch from the dry mechanical tests and the effective steady-state stretch measured from the free swelling experiments. The PDMS polymer was observed to have a higher steady-state stretch than the maximum locking stretch, which is presumed to be due to either an increase in locking length of the PDMS network when immersed in pentane, or compressibility of the polymer when swollen. This discrepancy warrants further investigation.

Bilayer strips, composed of a layer of 10:1 PDMS and 20:1 PDMS were immersed in pentane and allowed to swell to a steady-state geometry. Due to the higher volume uptake of the 20:1 PDMS compared to the 10:1 PDMS, the swollen shape of the bilayer strip is curved. The radii of curvature were measured for three experimental specimens and compared to finite-element simulations as a validation of the theory. The experimental and simulated radii of curvature were found to be in reasonably good agreement.

Some suggestions for future work are given next:

- The flexure swelling experiment should be executed with a higher imaging rate at the beginning of the experiment, when the swelling is extremely fast, to allow for better accuracy in the steady state region of the force curve.
- The bilayer experiment should also be repeated for different geometries and with better layer uniformity.
- The aforementioned discrepancy between the effective locking stretch measured in the dry mechanical tension experiments and the steady state effective stretch measured in the swelling experiments needs to be further investigated. One suggestion is to perform mechanical tests on samples which have been exposed to PDMS to see if the effective locking stretch has increased.

Appendix A

Free swelling and shrinking

To visualize the transient shape change of the cylindrical PDMS sample from its dry to swollen state, the PDMS was placed in a closed glass container and imaged every minute for 8 hours, from the side and from the bottom. The swelling over time is shown in Figure A-1. The cylindrical sample initially swells to a hyperboloid shape, and eventually returns to a cylindrical shape at steady state.

This process was also repeated in reverse, with a swollen PDMS sample left open to the air and imaged as it shrinks to the dry state. In this process, the cylindrical sample shape change is the opposite to the free swelling case, and the sides bulge outward until it arrives at its original cylindrical shape after all pentane has evaporated. The shrinking over time is shown in Figure A-2.

In some cases, due to the rapid evaporation of the pentane, the samples experienced very high tensile stresses on the surface that caused them to tear apart during the shrinking process. This is shown in Figure A-3.

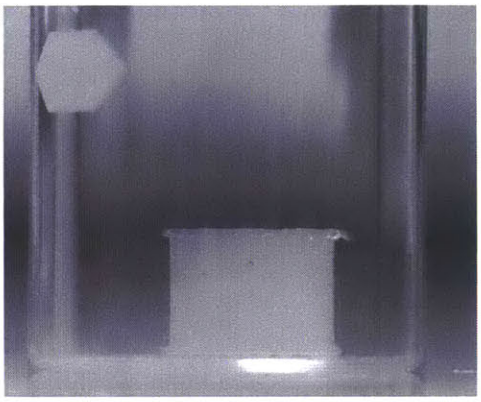

(a) Initial dry PDMS

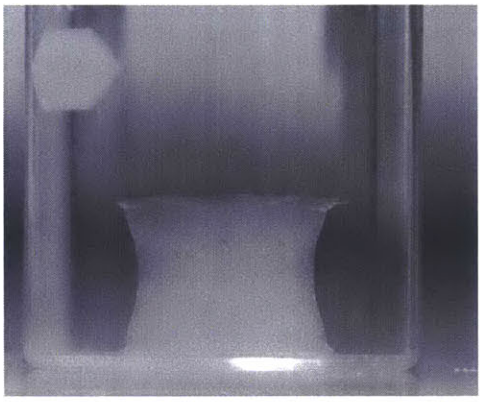

(b) 30 minutes

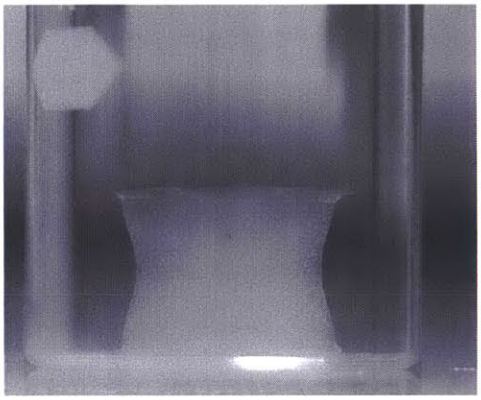

(c) 1 hour

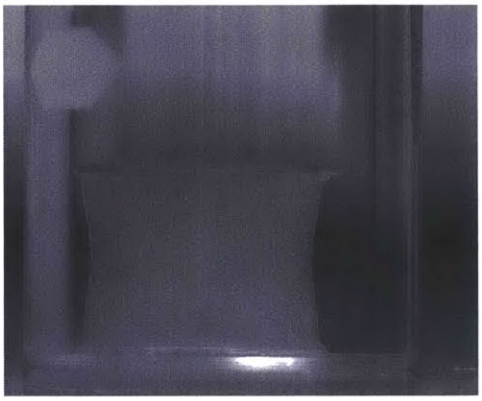

(d) 4 hours

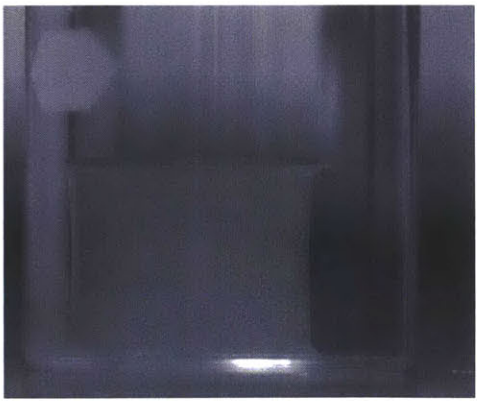

(e) 8 hours

Figure A-1: The free swelling experiment.

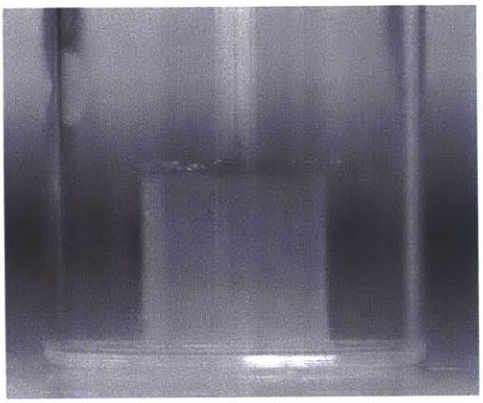

(a) Initial swollen PDMS

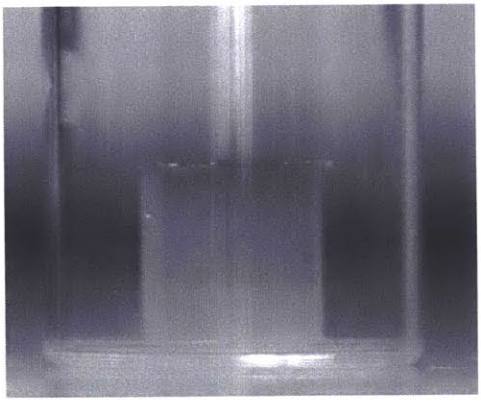

(b) 10 minutes

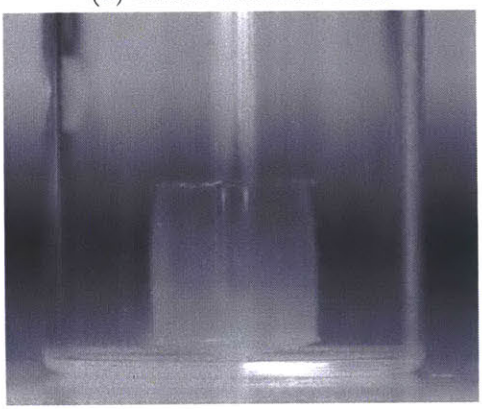

(c) 20 minutes

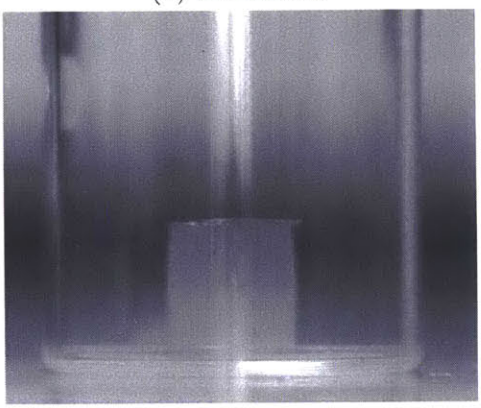

(d) 30 minutes

Figure A-2: The free shrinking experiment.

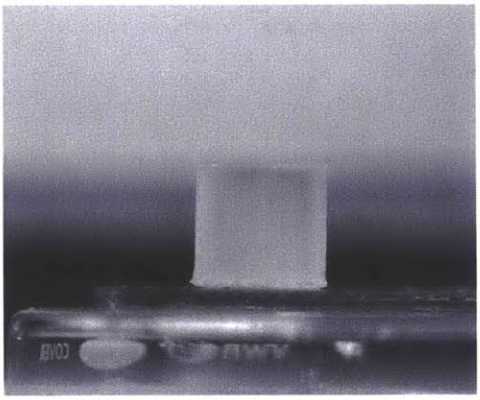

(a) Initial swollen PDMS

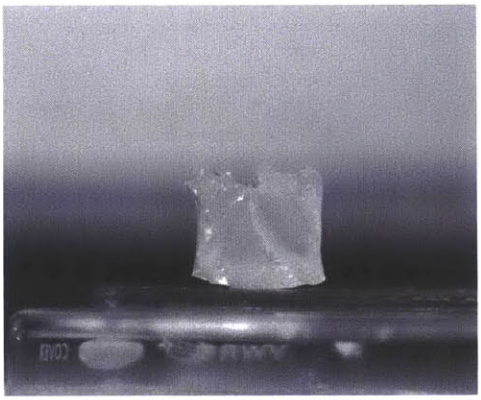

(b) 7 minutes

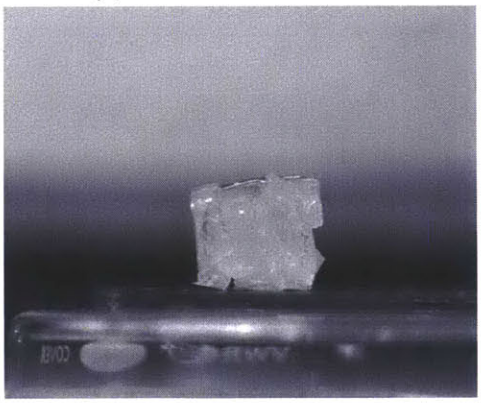

(c) 15 minutes

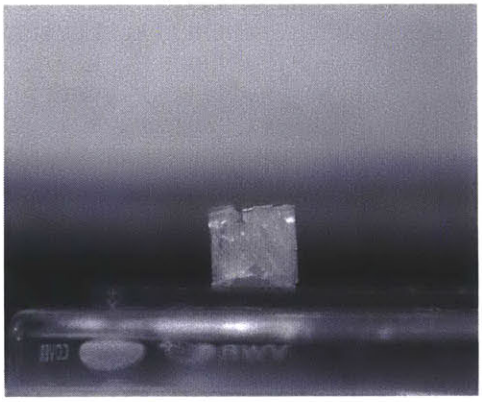

(d) 1 hour

Figure A-3: The free shrinking experiment, showing the high tensile surface stresses caused by the rapid evaporation rate of pentane.

Bibliography

S.A. Chester and L. Anand. A coupled theory for fluid permeation and large deformations for elastomeric materials. *Journal of the Mechanics and Physics of Solids*, 58:1879–1906, 2010.

S.A. Chester and L. Anand. A thermo-mechanically coupled theory for fluid permeation in elastomeric materials: Application to thermally responsive gels. *Journal of the Mechanics and Physics of Solids*, 59:1978–2006, 2011.

S.A. Chester, C.V. Di Leo, and L. Anand. A finite element implementation of a coupled diffusion-deformation theory for elastomeric gels. *International Journal of Solids and Structures*, 52:1–18, 2015.

Y. Hu, X. Chen, G.M. Whitesides, J.J. Vlassak, and Z. Sui. Indentation of polydimethylsiloxane submerged in organic solvents. *J. Mater. Res.*, 26:785–795, 2011.

R. Huang and L. Anand. Non-linear mechanical behavior of the elastomer polydimethylsiloxane (pdms) used in the manufacture of microfluidic devices. Technical report, Manufacturing Systems and Technology (IMST), 2005.

R. Huang and L. Anand. Non-linear elastic properties of poly(dimethylsiloxane) (pdms). Unpublished personal communication, 2015.

J.E. Mark. *Polymer Data Handbook*. Oxford University Press, 1998.

Sigma-Aldrich. Pentane safety data sheet, March 2015.